Electroencephalography and clinical Neurophysiology, 1986, 64: 123-143
Elsevier Scientific Publishers Ireland, Ltd.

Experimental Section

CORTICO-CORTICAL ASSOCIATIONS AND EEG COHERENCE: A TWO-COMPARTMENTAL MODEL

R.W. THATCHER, P.J. KRAUSE and M. HRYBYK

Applied Neuroscience Research Institute, University of Maryland Eastern Shore, Princess Anne, MD 21853, and University of Maryland School of Medicine, Baltimore, MD 21201 (U.S.A.)

(Accepted for publication: December 11, 1985)

Summary EEG coherence was computed from 19 scalp locations from 189 children ranging in age from 5 to 16 years. Tests of spatial homogeneity of EEG coherence were conducted by comparing EEG coherence as a function of different interelectrode distances in the anterior-to-posterior versus posterior-to-anterior directions. Highly significant inhomogeneities were observed since greater coherence was present in the anterior-to-posterior direction than in the posterior-to-anterior directions. Greater coherence was also present in frontal derivations than in posterior derivations and from the right hemisphere in comparison to the left hemisphere. These data indicate that at least two separate sources of EEG coherence were present (1) coherence produced through the action of short length axonal connections, and (2) coherence produced through the action of long distance connections. Measures of phase delays as a function of interelectrode distance supported the development of a 'two-compartmental' model of EEG coherence in which different features of coherence are produced by different length fiber systems. Based on this model a number of hypotheses were developed to explain differences in connectivity between left and right hemispheres and frontal versus occipital cortex.

Keywords: *EEG – coherence – cortico-cortical association – two-compartmental model*

The human electroencephalogram (EEG) reflects the ongoing rhythmical electrical activity of the brain. While electro-chemical synaptic events are accepted as the elementary EEG generators (Purpura 1959), the mechanisms by which synaptic potentials summate and neural generators are synchronized is largely unknown. Questions regarding the mechanisms of EEG frequency changes and the factors that determine the topographic distributions of wave amplitude and phase, which are characteristic of the human waking EEG, are still unanswered. A recent attempt to relate known cortical anatomical and physiological facts to the genesis of EEG was made by Nunez (1981), in which a non-linear mathematical wave model was developed that incorporated variables such as synaptic delays, conduction velocity and cortical association fiber lengths. This model, while valuable as a first attempt, still lacks empirical rigor concerning the distribution of local and long distance cortical association fibers as well as predictions of EEG synchrony based on the cortico-cortical associations. Such theoretical integration is important since advancements in our understanding of EEG and its clinical usefulness depend, in part, on the degree to which features of the human scalp EEG can be related to anatomical and physiological properties.

Standard EEG practice involves recording simultaneously from multiple areas of the scalp, and producing a set of time series measures of voltage. The frequency composition of the data from each channel can be determined by power spectral analyses and the covariance of spectral energies between any pair of channels at a particular frequency can be determined by coherence which is a measure of phase consistency or 'synchrony.' Measures of coherence are appearing in an increasing literature on electroencephalographic correlates of cognitive processing (Busk and Galbraith 1975; Shaw et al. 1977; Beaumont et al. 1978; Tucker et al. 1982; Thatcher et al. 1983) and as measures of abnormality in psychiatric and other areas of clinical medicine (Shaw et al. 1977; O'Conner et al. 1979; Cantor et al. 1982; Flor-Henry et al. 1982). Beaumont and Rugg (1979) argue that coherence offers advantages over power data, since coherence is less dependent on

reference electrode sites. Another advantage of coherence is its dependency on the spatial properties of a network, since both local and distant coupling between neural generators will be reflected in coherence. For example, in a homogeneous non-connected system, coherence would be modeled by random phase relations between distributed generators and thus would fall off with horizontal distance and it would be maximum at zero phase lag. Experimental evidence, however, suggests that human EEG coherence may, in fact, increase with horizontal separation and reach a maximum at large phase lags (Nunez 1981). This indicates the need to postulate functional links between widely separated regions of cortex using known facts about cortical anatomy.

Certain critical anatomical relations were considered in the present study. For example, anatomical analyses by Sholl (1956), Krieg (1963), Braitenberg (1974, 1978) and Szentágothai (1978) estimate that no more than 1% of the fibers that enter the cerebral cortex arise from the thalamus and approximately 2–4% of the fibers entering a hemisphere originate from the contralateral hemisphere (Nunez 1981). These analyses indicate that the majority of fibers (approximately 95%) entering the gray matter of the cortex arise from within the same hemisphere and that, in general, the input to one region of the cortex is the output from some other region. While inhibitory and excitatory 'inter-columnar' connections are short range, having an average length of less than 1 mm (Braitenberg 1978; Szentágothai 1978), the average length of cortico-cortical association fibers has been estimated to be several centimeters (Braitenberg 1978; Nunez 1981) and these fibers are believed to be exclusively excitatory (Szentágothai 1978). These estimates emphasize the need to incorporate the long-range cortico-cortical association system into any model which attempts to predict gross EEG cortical phenomena.

In the present paper a '2-compartmental' model is presented to explain EEG coherence. This model is based on the fact that the neocortex contains 2 classes of cells: (1) long axoned pyramidal or Golgi type I cells; and (2) short axoned stellate and Martinotti cells referred to as Golgi type II cells (Globus and Scheibel 1967; Szentágothai 1978). Approximately 75% of the cells in the human neocortex are pyramidal cells all of which have long axons (sometimes greater than 25 cm) that give off short length collaterals before the axon enters the white matter (Braitenberg 1972, 1978). In contrast, the Golgi type II cells have short axons (3–17 mm) that terminate in the local domain and do not enter the white matter. Due to the geometry of the isocortex, Golgi type II cells are believed to be responsible for a divergence pattern of connections (Braitenberg 1978) while the Golgi type I cells are responsible for long distance feedback loop connections (e.g., fronto-occipital fasciculi; Carpender and Sutin 1983).

Given the fact that the axonal density per unit volume of cortex is approximately 10–100 times higher for Golgi type II cells than Golgi type I cells (Braitenberg 1978), it is expected that the shorter the distance between scalp electrodes the greater the contribution to coherence by short distance axonal connections. Since the density of short axon connections between any two regions of cortex falls off with distance, one would expect a curvilinear or quadratic relationship to exist between coherence and the separation distance between electrodes. This is because at long electrode separations the contribution to coherence by short axon connections would be minimal while contributions by long axon connections would increase. Finally, given the presence of long cortical fasciculi and regional specificity of connections (Carpender and Sutin 1983) it must be assumed that the cortex is not spatially homogeneous (i.e., is anisotropic) and, therefore, if coherence indeed reflects cortical connectivity then it should reflect this anisotropy in a manner that corresponds with known anatomical connections.

In the present study the EEGs from 189 children were analyzed using 2 different methods: (1) comparisons of mean coherence as a function of electrode separation for different frequency bands, and (2) multivariate and bivariate regression analyses in which the relative contribution due to local axonal connections was minimized. Questions of particular interest were: (1) to what extent does the magnitude of coherence vary with spatial separation; (2) are there differences in the magnitude of coherence within the left hemisphere in com-

parison to within the right hemisphere; (3) to what extent are measures of coherence spatially inhomogeneous (anisotropic); (4) to what extent does the magnitude of coherence vary as a function of EEG frequency; and (5) are there patterns of coupling between specific regions of the scalp?

Methods

(A) Subjects

In 1979, a total of 200 subjects were recruited as part of a USDA study of the relations between nutrition and brain development in rural children (Thatcher et al. 1983). The children were enrolled in the public school systems of the rural eastern shore of Maryland and they were recruited by newspaper advertisements as well as through cooperative arrangements with the Somerset County Board of Education. From this group of 200 children the data of 11 children were excluded: one child who had suffered severe neurological damage, three with a full-scale WISC-R of less than 60, and seven whose EEGs were lost due to technical problems. The 189 subjects included in this study (87 female, 102 male) were aged 5.0–17.7 with the mean age = 10.141 and S.D. = 2.879. The children were given the Wechsler Intelligence Test for Children (Wechsler 1974). The range of full-scale I.Q. of the children in this study was from 65 to 150 with a mean of 108.01 and an S.D. of 16.69.

(B) Electrophysiological data analyses

Grass silver disk electrodes were applied to the 19 scalp sites of the international 10/20 system (Jasper 1958). A transorbital eye channel (electrooculogram or EOG) was used to measure eye movements. All scalp recordings were referenced to linked ear lobes. Amplifier bandwidths were nominally 0.5–30 Hz, the outputs being 3 dB down at these frequencies. The EEG activity was digitized on-line by a PDP 11/03 data acquisition system. An on-line artifact rejection routine was used which excluded segments of EEG if the voltage in any channel exceeded a preset limit determined at the beginning of each session to be typical of the subject's resting EEG and EOG.

A maximum of 1 min of eyes-closed artifact-free EEG was obtained at a digitization rate of 100 Hz with the subject's eyes closed. The EEG segments were analyzed by a PDP 11/70 computer and plotted by a Versatec printer/plotter. Each subject's EEG was then visually examined and edited to eliminate any artifacts that may have passed through the on-line artifact rejection process.

A second-order recursive digital filter analysis was used to compute the auto- and cross-spectral power density (Otnes and Enochson 1972) for each channel. This procedure is essentially identical to the Fast Fourier Transform (FFT) method of computing power spectral density. The advantage of the recursive digital filter, when a limited number of bands are analyzed, is increased computational efficiency and a simpler design, since the recursive filters provide a natural form of windowing and leakage suppression. The procedure involved using a first difference pre-whitening filter: $y(i) = x(i) - x(i-2)$ and a 2-stage (4-pole) Butterworth bandpass filter (for mathematical equations see Otnes and Enochson 1972). Frequency bands, including the center frequencies (fc) and 1/2 power values (B) were: delta (0.5–3.5 Hz; fc = 2.0 Hz and B = 1.0 Hz), theta (3.5–7.0 Hz; fc = 4.25 Hz and B = 3.5 Hz), alpha (7.0–13.0 Hz; fc = 9.0 Hz and B = 6.0 Hz); beta (13–22 Hz; fc = 19 Hz and B = 14.0 Hz). Degrees of freedom = 2 BwT, where Bw = the bandwidth and T the length of the record (e.g., for 20 sec of EEG there are 160 degrees of freedom) and the start-up and trail-off periods of the filter are 2/Bw sec or 0.5 sec for a 4 Hz bandwidth (Otnes and Enochson 1972). The artifacting routines precluded EEG segments less than 0.8 sec in length and the range of total EEG length/subject varied from 16 sec to 60 sec (mean = 42 sec, S.D. 13.61). Coherence is defined as

$$\gamma^2_{xy}(f) = \frac{(G_{xy}(f))^2}{(G_{xx}(f)G_{yy}(f))}$$

where $G_{xy}(f)$ is the cross-power spectral density and $G_{xx}(f)$ and $G_{yy}(f)$ are the respective auto-power spectral densities (Otnes and Enochson 1972; Glaser and Ruchkin 1976). Coherence was computed for all pairwise combinations of the following 16 channels (O1, O2, P3, P4, T5, T6, T3,

T4, C3, C4, F3, F4, F7, F8, Fp1, Fp2) for each of the 4 frequency bands. The computational procedure to obtain coherence involved first computing the power spectra for x and y and then the normalized cross-spectra. Since complex analyses are involved this produced the cospectrum ('r' for real) and quadspectrum ('q' for imaginary). Then coherence was computed as:

$$\gamma^2_{xy} = \frac{r^2_{xy} + q^2_{xy}}{G_{xx}G_{yy}}$$

and the phase difference, in milliseconds, was computed as: phase = 159.1549 tan -1 (q/r)/SC, where SC is the center frequency of the recursive filter. A radius vector or resultant was derived at the phase shift at which there was maximum coherence (Otnes and Enochson 1972).

(C) Statistical analyses

BMDP Biomedical Statistical Programs (Dixon and Brown 1979) were used for all analyses. Distributions and descriptive statistics were computed for each variable, using BMDP2D and BMDP7D. These measures included histograms, arithmetic means, standard deviations, variance, skewness, kurtosis and the coefficient of variation. In order to obtain gaussian distributions the coherence measures were transformed according to $\log \frac{x}{100-x}$. These analyses revealed that all variables approximated the normal distribution.

Polynomial regression (BMDP5R) analyses were conducted first in order to determine whether the relationships between coherence variables were linear or non-linear. Once linearity versus non-linearity was assessed, stepwise, hierarchical regression (BMDP2R) analyses were conducted. In some analyses a partial coherence function was computed by forcing in contralateral hemispheric coherence variables before entry of the ipsilateral coherence variables. In this analysis, the intercorrelation of the contralateral variables was removed before entry of the ipsilateral variables and, thus, the partial coherence between two or more intrahemisphere coherence measures was assessed, independent of contralateral coherence. This procedure is similar to the hermetian matrix method of computing partial coherence (Otnes and Enochson 1972) as well Tucker and Roth's (1984) application of this technique to EEG. In other analyses, unforced stepwise entry of variables occurred in which the order of entry was determined by the strength of correlation between the independent and dependent variables. However, there were no major differences in the outcome or the interpretation of the results using these different methods, and therefore only the results of the unforced stepwise regression procedure is reported.

Results

Spatial analyses of coherence

Based on volume conduction, if we assume that there is spatial homogeneity in a non-connected system then one would expect coherence to exhibit a smooth decrement with increased electrode separation. Further, this decrement should be equal for anterior-to-posterior versus posterior-to-anterior directions. In order to test this model, coherence was measured along two parallel lines with scalp electrodes equally spaced according to the international 10/20 convention (Jasper 1958). In Fig. 1, the mean separation distance between adjacent electrode pairs was calculated to be 6.79 cm (or approximately 7 cm). This value was calculated by computing the mean inion to nasion distance for the population of 189 children and multiplying by 0.2 in order to approximate the average 10/20 electrode distance (Jasper 1958), or $\mu = (33.9 \text{ cm})\ (0.2) = 6.79$ cm. Fig. 2 shows the results of a test of the assumptions, in which mean coherence values are plotted as a function of increasing interelectrode separation distance. Four curves were generated for each EEG frequency, two for the anterior-to-posterior direction (i.e., Fp1-Fp3, Fp1-C3, Fp1-P3, Fp1-O1 and Fp2-F4, Fp2-C4, Fp2-P4, Fp2-O2) and two for the posterior-to-anterior direction (O1-P3, O1-C3, O1-F3, O1-Fp1 and O2-P4, O2-C4, O2-F4, O2-Fp2). It can be seen that in all instances there was greater mean coherence in the anterior-to-posterior direction than in the posterior-to-anterior direction (delta $F = 34$, $P < 0.00001$; theta $F = 81.9$, $P < 0.00001$; alpha $F = 173$, $P < 0.00001$; beta $F = 80.8$, $P < 0.00001$). In addition, the right hemi-

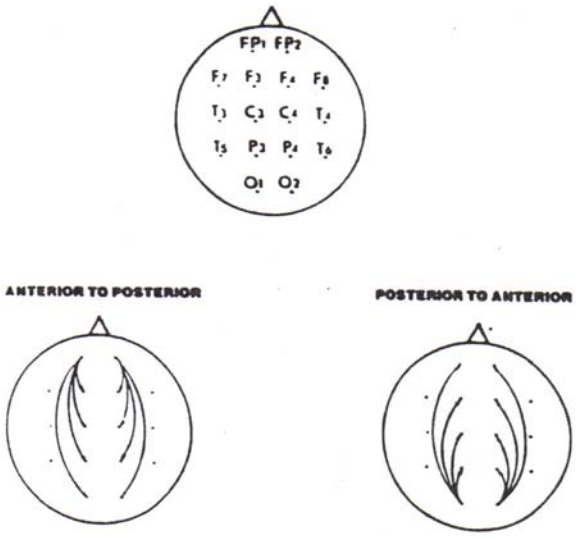

Fig. 1. Diagrammatic representation of the anterior-to-posterior and posterior-to-anterior location of scalp electrodes.

sphere derivations exhibited greater mean coherence than homologous left hemisphere derivations ($F = 10.758$, $df = 1/188$, $P < 0.00001$). The right hemisphere coherence was greater than left hemisphere coherence in 30 out of the 32 comparisons. A non-parametric sign test of left versus right hemisphere mean coherence was significant at $P < 0.00001$.

The observed differences in directionality (anterior-to-posterior versus posterior-to-anterior) as well as differences between left and right hemispheres are indicative of a non-isotropic distribution of local and/or long distance fibers. In order to examine the nature of this presumed non-isotropy, polynomial regression analyses (BMDP5R) were performed on the data points in Fig. 2. These analyses involved first interpolating between each point using a spline interpolation algorithm. Coherence was the dependent variable

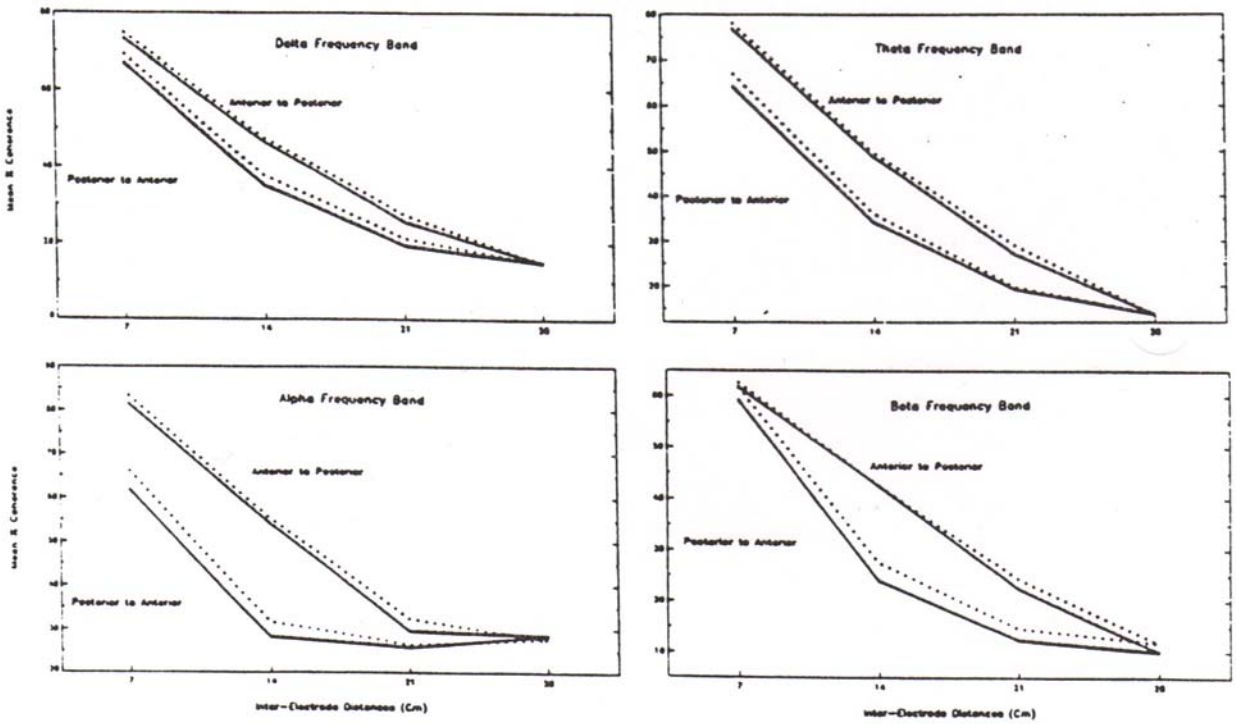

Fig. 2. Mean percent coherence in the anterior-to-posterior and posterior-to-anterior direction for increasing interelectrode distances. 'A' represents the mean percent coherence versus interelectrode distance in the delta frequency band, 'B' for the theta frequency band, 'C' for the alpha frequency band and 'D' for the beta frequency band. Dotted lines represent the right hemisphere and solid lines are values from the left hemisphere.

and distance the independent variable. The results of the polynomial regression analyses showed that the curves were described best by a quadratic regression equation. Terms higher than the quadratic were not significant. Analyses of the slopes of the regression equations as well as the differences in mean coherence between 7 and 14 cm, 14 and 21 cm, 21 and 28 cm demonstrated significantly steeper negative slopes in the posterior-to-anterior direction than in the anterior-to-posterior direction. Table I shows that the differences in slope were most pronounced in the posterior-to-anterior direction. These results show that 2 forms of spatial inhomogeneity were present in both hemispheres: (1) there was significantly greater mean coherence in the anterior-to-posterior direction than from measures in the posterior-to-anterior direction, and (2) the rate of fall-off with distance was significantly greater in the posterior-to-anterior direction than in the anterior-to-posterior direction.

The examples of spatial inhomogeneity in mean coherence shown in Fig. 2 were present in all 4 frequency bands. However, it is also important to determine whether there are spatial inhomogeneities in coherence at different frequencies. Analyses of the observed differences in coherence at different frequencies at different electrode separations are shown in Fig. 3. It can be seen that there is a consistent peak in coherence in the alpha band in the anterior-to-posterior direction. In contrast, there is no peak coherence in the posterior-to-anterior direction in the alpha band at 7 and 14 cm. However, at 21 and 28 cm a peak in coherence in the alpha band is present in both the posterior-to-anterior separations as well as in the anterior to-posterior separations. This is a further example of spatial inhomogeneity, in which the relative amount of coherence in different EEG frequency bands varies depending on the direction of electrode separation. These differences cannot be explained by volume conduction since the distances are the same magnitude in both directions, and in the case of 14 cm, a common electrode (e.g., C3 and C4) is shared in the posterior-to-anterior and anterior-to-posterior directions.

Polynomial regression analyses

The previous analyses demonstrated considerable inhomogeneity in the spatial distribution of EEG coherence recorded from the scalp. These data are consistent with a dual compartment model of coherence which argues that both short distance and long distance cortical axonal fibers contribute to cortical coherence. For example, the sharp fall off in coherence with distance in Fig. 2 and the relatively weak quadratic form of the curves is indicative of a strong contribution by local fiber systems. Since volume conduction and local fiber connections may mask the contributions to coherence by long fiber systems efforts were made to minimize their effects. A technique which minimizes the contribution of local coherence is the bivariate polynomial regression analysis. In this analysis, the covariance between local coherence from one region of the scalp and local coherence recorded from a distant region is examined. The hypothesis is that contributions by local factors tend to be minimized when covariance is evaluated between two 'local' regions (e.g., 7 cm)

TABLE I

Analyses of variance of the slope (rate of change) of coherence with distance. In all cases the rate of change with interelectrode distance was greater in the posterior-to-anterior direction than in the anterior-to-posterior direction.

	Left hemisphere slopes						Right hemisphere slopes					
	O1-P3		Fp1-F3		*F*	*P*	O2-P4		Fp2-F4		*F*	*P*
	Mean	S.D.	Mean	S.D.			Mean	S.D.	Mean	S.D.		
Delta	−4.62	1.52	−3.86	1.71	20.35	0.00001	−4.57	1.97	−3.95	1.59	10.84	0.0011
Theta	−4.39	1.62	−4.01	1.60	13.39	0.0264	−4.45	1.75	−4.09	1.62	11.74	0.0430
Alpha	−4.81	2.29	−3.89	2.15	15.56	0.0001	−4.93	2.27	−3.99	2.10	16.56	0.0001
Beta	−5.15	1.67	−2.88	1.70	166.45	0.0000001	−4.98	1.68	−3.04	1.64	123.49	0.00000001

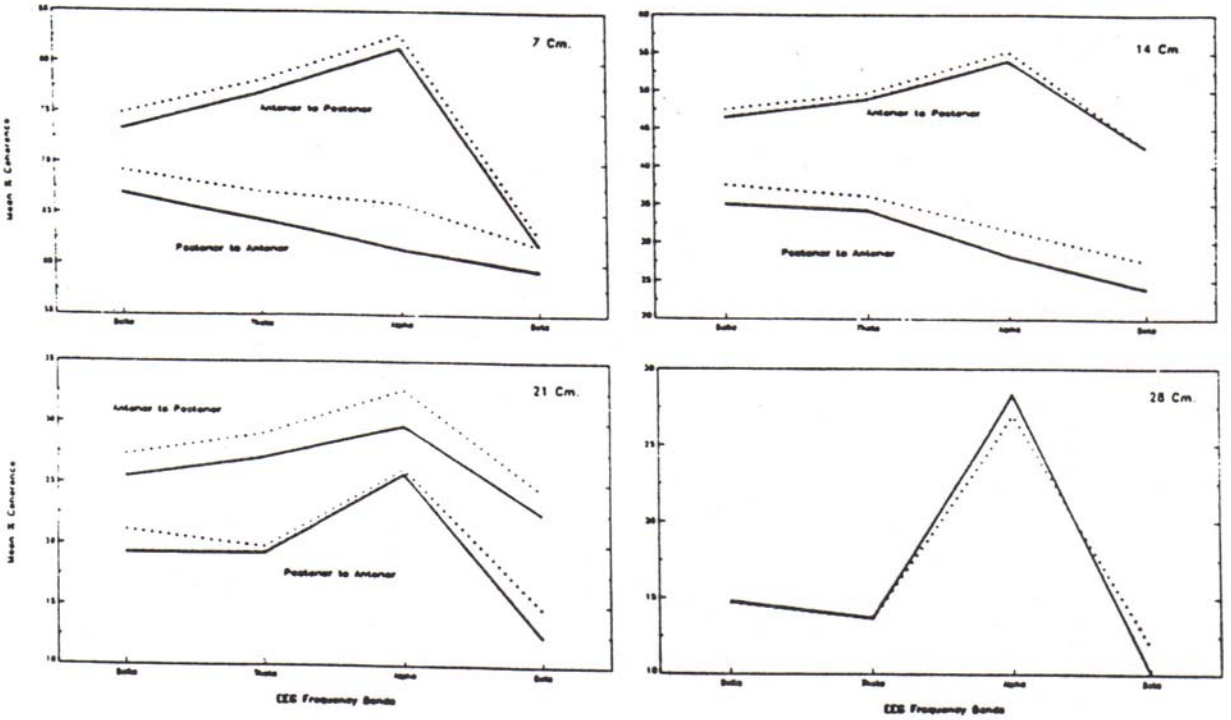

Fig. 3. Mean percent coherence in the anterior-to-posterior and posterior-to-anterior direction at different EEG frequency bands. 'A' represents the mean percent coherence versus EEG frequency at 7 cm interelectrode distances, 'B' for 14 cm interelectrode distances, 'C' for 21 cm interelectrode distances and 'D' for 28 cm interelectrode distances. Dotted lines represent the right hemisphere and solid lines are values from the left hemisphere.

which are separated by a longer distance (e.g., 28 cm). For example, the covariance between O1-P3 coherence and F3-F4 coherence is likely to be due to the long distance connections linking these widely separated locations, especially when there is less covariance from intermediate locations.

In order to test this notion, polynomial regression analyses (BMDP5R) were conducted in which 7 interhemispheric coherence measures were the dependent variables (i.e., O1/O2; P3/P4; C3/C4; T3/T4; T5/T6; F7/F8; F3/F4) and 10 intrahemispheric local coherence measures were the independent variables (i.e., O1/P3; P3/C3; T3/T5; C3/F3; T3/F7; O2/P4; P4/C4; T4/T6; C4/F4; T4/F8). Table II shows the results of these analyses. A total of 280 separate tests were conducted, of these 197 (or 70.4%) were statistically significant ($P < 0.05$). Of the statistically significant tests, only 13.2% were significantly quadratic without a significant linear term and there were only 3 significant third- and/or fourth-order terms. Nonetheless, 38.1% of the significant tests in Table II contained both a linear and a non-linear term (quadratic) while only 47.7% were exclusively linear.

Evidence for the contribution of long association fibers is present in Table II in which intrahemispheric coherence in posterior regions (O1-P3 and O2-P4) predicts interhemispheric coherence in frontal regions (F3-F4). In contrast to F3-F4, interhemispheric coherence in O1-O2 and C3-C4 is related almost exclusively to coherence in surrounding or local intrahemispheric regions. This indicates that there are at least two determiners of coherence: (1) local connections, and (2) distant connections. In the cases of O1-O2 and C3-C4 the effect of local or neighboring connections is dominant, while in the case of F3-F4 long distant connections dominate.

Thus, the polynomial regression analyses dem-

onstrate a marked spatial inhomogeneity as well as patterns of covariance between different scalp regions. However, the contribution by volume conduction necessarily overlaps the underlying contribution by specific fiber systems. While digital signal processing techniques may help subtract

TABLE II

't' values ($P < 0.05$) from polynomial regressions in which interhemispheric coherence is the dependent variable and intrahemispheric coherence is the independent variable.

	Delta		Theta		Alpha		Beta	
	Linear	Quad	Linear	Quad	Linear	Quad	Linear	Quad
Dependent variable = O1-O2								
O1/P3	6.57	4.83	5.44	4.06	2.87	3.66	2.29	4.59
O2/P4	6.79	5.66	6.38	4.36	2.52	4.13	5.02	3.33
P3/C3	4.60	-	2.94	-	-	-	2.85	-
P4/C4	3.02	2.98	3.15	-	-	-	2.54	-
T5/T3	3.62	-	2.86	-	-2.53	-	-	-
T6/T4	3.20	-	2.99	-	-2.85	-	3.62	2.03
C3/F3	-	-	-	-	-	-	-	-
C4/F4	-	-	-	-	-	-	-	-
T3/F7	2.06	-2.17	2.55	-2.40	2.68	-	3.17	-
T4/F8	-	-	-	-	-	-	2.87	-
Dependent variable = C3-C4								
O1/P3	4.35	3.59	-	2.07	-	-	-	-
O2/P4	2.71	3.71	2.35	2.19	-	-	-	-
P3/C3	9.26	2.44	6.27	-	3.82	2.72	7.50	-
P4/C4	7.25	2.17	6.48	2.08	2.41	-	6.71	-
T5/T3	4.33	-	-	-	-	-	-	-
T6/T4	5.14	-	3.11	-	-	-2.54	2.90	-
C3/F3	5.63	-	6.77	2.12	13.13	3.19	7.41	2.82
C4/F4	5.73	2.07	8.06	-	13.87	3.45	10.34	-
T3/F7	-	-	2.81	-	5.18	2.05	-	-
T4/F8	-	2.07	3.44	3.21	4.54	-	4.85	2.27
Dependent variable = F3-F4								
O1/P3	5.59	-3.76	4.07	-3.81	3.27	-2.74	3.35	-3.16
O2/P4	8.47	-6.00	5.43	-7.71	2.52	-	3.80	-2.10
P3/C3	2.67	-	2.37	-	-	-	2.66	-
P4/C4	2.35	2.32	-	3.59	-	-	3.45	-
T5/T3	-	-	-	-	-	-	-	-
T6/T4	2.68	-	-	-	-	-	4.93	-2.46
C3/F3	3.79	-	2.21	-	-	3.87	7.56	-
C4/F4	2.07	-	2.63	-	-	2.83	6.27	-
T3/F7	3.14	-	2.43	-	4.36	-	3.81	-
T4/F8	-	-	2.73	-	-	2.83	5.67	-
Dependent variable = P3-P4								
O1/P3	9.49	-	7.61	-	3.44	-	3.44	-
O2/P4	11.66	-	7.78	-3.51	3.28	-	3.28	-
P3/C3	6.50	-	6.15	-	2.46	-	2.46	-
P4/C4	5.86	3.20	5.37	2.29	-	-	-	-
T5/T3	4.76	-	4.12	-	-	-	-	-
T6/T4	5.61	-	3.83	-	-	-2.96	-	-2.96
C3/F3	3.39	-	2.00	-	4.00	2.11	4.00	2.11
C4/F4	2.32	2.62	2.48	-	4.91	-	4.91	-
T3/F7	2.41	-	-	-	3.74	-	3.74	-
T4/F8	-	-	-	-	-	-	-	-

TABLE II (continued)

	Delta		Theta		Alpha		Beta	
	Linear	Quad	Linear	Quad	Linear	Quad	Linear	Quad
Dependent variable = T5-T6								
O1/P3	6.29	4.20	3.27	4.06	4.15	3.32	4.15	3.32
O2/P4	6.12	5.60	4.76	3.26	4.05	2.76	4.05	2.76
P3/C3	6.01	2.30	4.57	-	-	2.94	-	2.94
P4/C4	5.38	2.61	4.63	2.08	-	-	-	-
T5/T3	5.06	-	2.80	-	-	2.28	-	2.28
T6/T4	5.68	2.37	3.67	2.67	-	2.03	-	2.02
C3/F3	2.57	-	2.91	-	-	-	-	-
C4/F4	2.53	-	-	-	-	-	-	-
T3/F7	-	-	-	-	2.08	-	2.08	-
T4/F8	-	-	-	-	-	-	-	-
Dependent variable = T3-T4								
O1/P3	-	2.42	-	-	-	-	-	-
O2/P4	2.58	-	-	-	-	-	-	-
P3/C3	6.01	-	3.09	-	-	-	-	-
P4/C4	4.68	3.36	3.28	4.06	2.65	-	2.65	-
T5/T3	3.27	-	-	-	-	-	-	-
T6/T4	5.10	-	2.35	-	-	-	-	-
C3/F3	2.28	-	4.13	-	2.91	2.84	2.91	2.84
C4/F4	2.69	1.99	2.85	2.14	-	3.03	-	3.03
T3/F7	-	-	2.01	-	4.74	4.33	4.74	4.33
T4/F8	3.18	-	3.14	2.68	2.87	4.18	2.87	4.18
Dependent variable = F7-F8								
O1/P3	-	-	-5.44	-	-	-	-	-
O2/P4	-	-	-	-	-	-	-	-
P3/C3	-	-	-	-	-1.96	3.37	-1.96	3.37
P4/C4	-	-	-	4.40	-	2.85	-	-
T5/T3	-	-	-3.67	-	-2.76	-	-2.76	-
T6/T4	-	2.81	-	2.50	-	2.43	-	2.85
C3/F3	2.30	2.68	3.56	-	2.38	4.18	2.38	4.18
C4/F4	-	-	2.22	-	-	2.81	-	2.43
T3/F7	-	-	-	-	4.84	2.16	4.84	2.16
T4/F8	2.03	2.34	3.97	-	3.48	4.49	-	2.81

Level of significance for two-tailed tests:
$P < 0.05 = (t > 1.96 < 2.31)$
$P < 0.01 = (t > 2.58 < 3.29)$
$P < 0.001 = (t > 3.29 < 3.89)$
$P < 0.0001 = (t > 3.90 < 4.56)$

common variance, a simple bivariate regression analysis is capable of revealing important features of the dynamics of closely coupled systems that digital signal processing may miss (Dudley 1977). For example, Fig. 4 shows examples of different types of linear and quadratic relationships from the polynomial regression analyses (in Table II). The most common linear relationship was the positive linear (Fig. 4A) and the most common quadratic was the positive linear with a positive quadratic (Fig. 4B). The positive linear relationship indicates that as coherence increases in the interhemispheric region, coherence also increases in the intrahemispheric region. The positive linear-positive quadratic indicates that at the lower range of coherence the degree of coupling between local regions is negligible, but that the coupling increases as coherence increases. While the posi-

tive linear and positive quadratic relationships represented 90% of the significant polynomial regressions. the 10% that were negative linear and/or negative quadratic are important, since negative relationships are often indicative of a competitive type of mechanism. For example, in Fig. 4C the negative linear relationship indicates that as coherence increases in the interhemispheric region. coherence decreases in the intrahemispheric region. This is indicative of a competitive relationship where increased coherence in one region of the cortex is at the expense of coherence elsewhere in the cortex. The negative quadratic (Fig. 4D) indicates a competitive relationship at the lower range of coherence with a limit reached near the asymptote in which the intrahemispheric and interhemispheric regions are no longer coupled.

Multivariate regression analyses

Given the abundance and complexity of cortical associations it is very likely that any two regions of the brain are covariant due to their connections to a third region of the brain. Therefore, patterns that may be observed in a univariate analysis, such as the polynomial regression analyses (Table II and Fig. 4), may not be present when the intercorrelations between independent variables are adjusted out of the regression equation. To examine this possibility, stepwise multiple regression analyses (BMDP2R) were performed. Either interhemispheric or intrahemispheric coherence was the dependent variable and, in separate analyses, all left intrahemispheric coherence variables and all right intrahemispheric coherence variables were the independent variables. In the stepwise procedure the order in which these predictor variables were entered into a regression equation was determined by their ability to account for the variance in the dependent variable that remained after each step, with the unentered variables at each step being adjusted for their partial correlation with the variables previously entered.

Fig. 5 shows the results of the interhemispheric regression analyses when O1-O2, C3-C4 and F3-F4 are the dependent variables. It can be seen that the anatomical patterns observed in the polynomial regression analyses (Table II) were basically unchanged. That is, the best predictor of O1-O2 interhemispheric coherence was occipital-parietal intrahemispheric coherence with little association with more anterior regions. For C3-C4 interhemispheric coherence, the central and frontal intrahemispheric coherence was the best predictor while regions anterior or posterior to the central areas exhibited less association. In contrast to the occipital and central interhemispheric coherence, F3-F4 coherence was predicted most strongly by occipital-parietal scalp regions. These results indicate that coherence in the medial frontal regions is strongly influenced by long association connections with posterior regions. Furthermore, this association is not bidirectional in that F3-F4 interhemispheric coherence covaries with posterior intrahemispheric coherence, but O1-O2 interhemispheric coherence does not covary with frontal intrahemispheric coherence. These findings can be explained if it is assumed that posterior and central coherence is dominated by local connections while medial frontal interhemispheric coherence is dominated by long distance connections. Medial frontal cortex is emphasized here because later frontal regions (i.e., F7, F8) failed to show strong posterior cortical relations.

Fig. 6 shows the results of topographic regression analyses for the intrahemispheric dependent variables. The analyses show that certain preferred coherence relationships are present. Presumably, these preferred relationships reflect an underlying connectivity. For example, local regions are often more strongly covariant with distant regions than with neighboring regions. Further, evidence of a preferred relationship to posterior-temporal regions (i.e., T5-T3 and T6-T4) is present since nearly every local intrahemispheric site was associated with the posterior-temporal regions and no other locations were as consistently associated as were the posterior-temporal regions. With the exception of the parietal-occipital locations, there was consistently greater variance accounted for by right hemisphere variables than by left hemisphere variables. Analyses of variance demonstrated a statistically greater percent variance accounted for from the right hemisphere in comparison to the left ($F = 215.58$, $df = 1/4$, $P < 0.00001$).

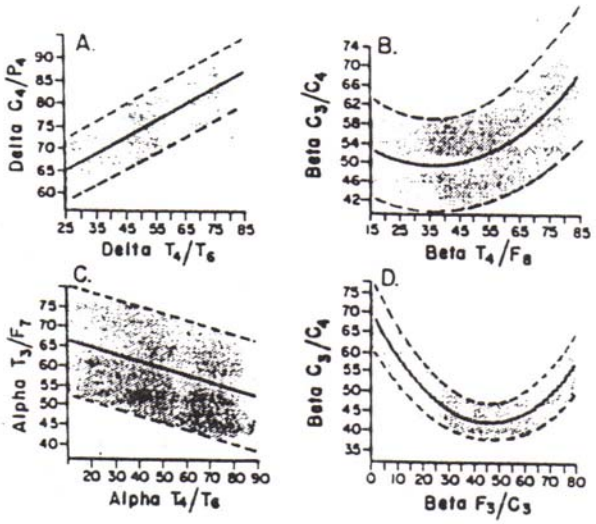

Fig. 4. Representative examples of the results of polynomial regression analyses. These analyses demonstrated different types of covariance between coherence recorded from different scalp locations. 'A' is an example of a positive linear relationship without significant higher order effects, 'B' is an example of a positive linear and positive quadratic relationship, 'C' is an example of a negative linear relationship without significant higher order effects and, 'D' is an example of a negative linear with a positive quadratic relationship.

Phase versus interelectrode distance

If we assume that coherence is a function of both short and long distance fibers, than one would predict that short and long fiber contributions can be distinguished by their relative phase contributions. Mathematically, phase in a connected system is a function of frequency, distance and conduction velocity; i.e.,

$$\Theta_{xy} = \frac{2\pi fd}{c},$$

where Θ_{xy} is the phase between locations x and y, f is the frequency in grads, d is the distance traveled in meters and c is the conduction velocity in m/sec (Bendat and Piersol 1980). If volume conduction in a non-connected system were the sole determiner of coherence, then no change in phase should occur over distance. On the other hand, if we assume that a uniform set of cortico-cortical association fibers are responsible for coherence, then a smooth increase in phase should occur as a function of distance. Finally, if two different fiber systems are responsible for coherence, then we would expect a non-linear or non-uniform increase in phase as a function of distance. Before conducting the analysis, a predic-

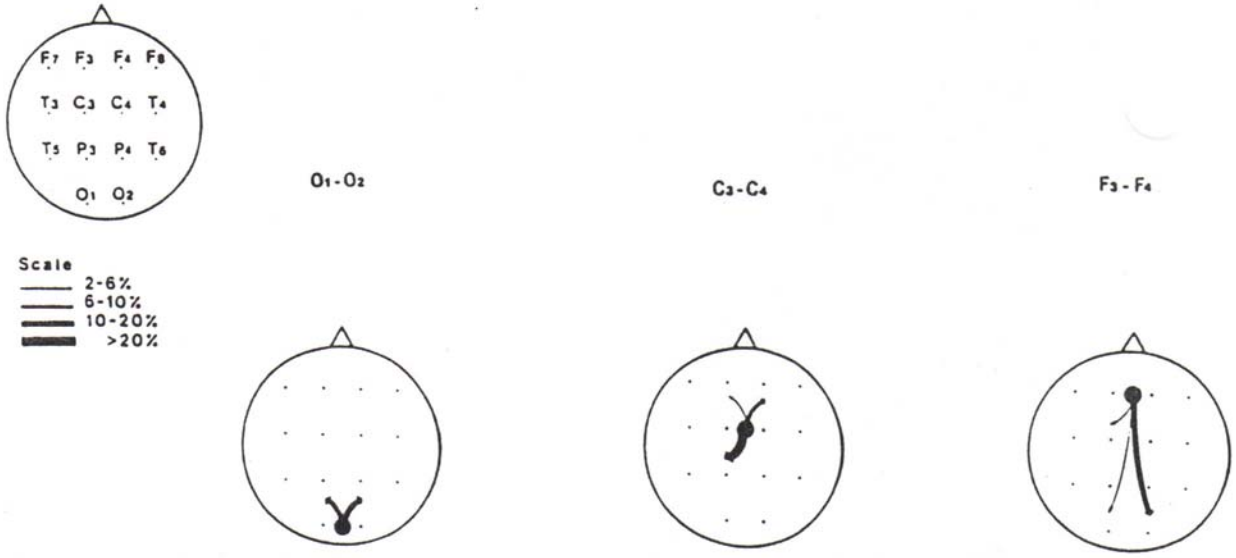

Fig. 5. A topographic representation of the results of stepwise regression analyses (BMDP2R) in which interhemispheric coherence at either O1-O2 or C3-C4 or F3-F4 was the dependent variable and intrahemispheric coherence (O1-P3; O2-P4; P3-C3; P4-C4; T5-T3; T4-T6; T3-F7; T4-F8; C3-F3; C4-F4) were the independent variables. The degree of association or R^2 between the independent variables (intrahemispheric coherence) and the dependent variable (interhemispheric coherence) is represented by the thickness of the lines connecting topographic locations. These results were obtained independent of age, sex and head circumference.

Regression Analyses of Intrahemispheric Coherence

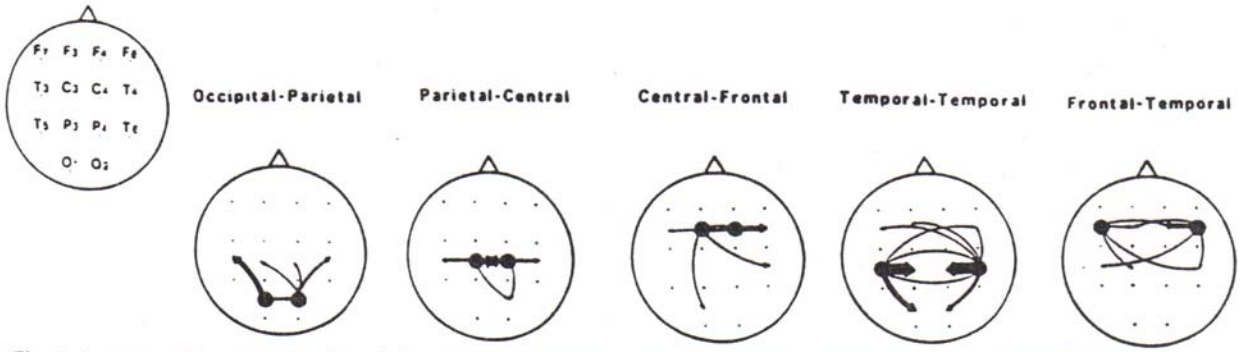

Fig. 6. A topographic representation of the results of stepwise regression analyses in which one of the intrahemispheric coherence locations was the dependent variable and the remainder of the intrahemispheric coherence locations were entered as independent variables. The degree of association or R^2 between the independent variables and the dependent variable is represented by the thickness of the lines connecting topographic locations. These results were obtained independent of age, sex and head circumference.

tion was made that the function relating phase to interelectrode distance should contain a relatively constant component which reflects volume conduction and contributions due to local fiber connections (e.g., 7 and 14 cm) and a non-linear (e.g., quadratic) compartment which reflects the contribution due to long distance fiber systems (e.g., > 14 cm).

Mean Abs Phase (Msec)

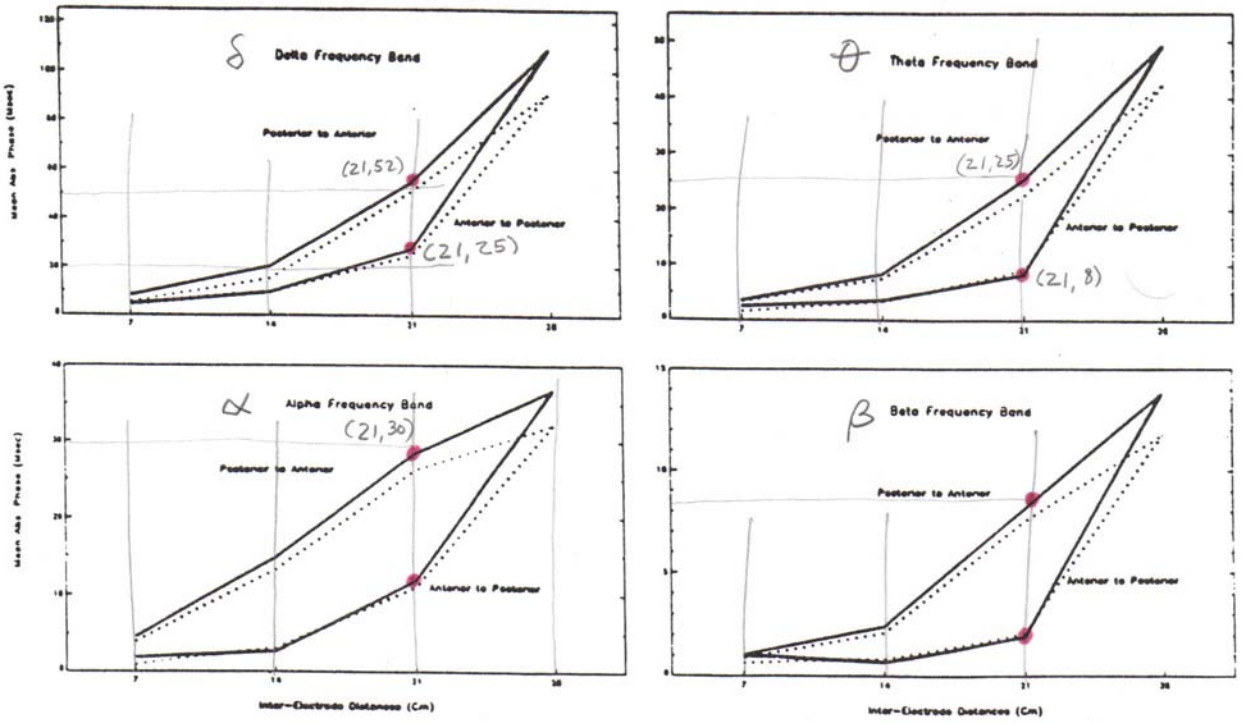

Fig. 7. Mean absolute phase (msec) in the anterior-to-posterior and posterior-to-anterior direction for increasing interelectrode distances. 'A' represents the mean absolute phase versus interelectrode distance in the delta frequency band, 'B' for the theta frequency band, 'C' for the alpha frequency band and 'D' for the beta frequency band. Dotted lines represent the right hemisphere and solid lines are values from the left hemisphere.

TABLE III

Analysis of variance on the slope (rate of change) of phase with distance. In all cases the rate of change with interelectrode distance was greater in the posterior-to-anterior direction than in the anterior-to-posterior direction.

	Left hemisphere slopes						Right hemisphere slopes					
	O1-P3		Fp1-F3		F	P	O2-P4		Fp2-F4		F	P
	Mean	S.D.	Mean	S.D.			Mean	S.D.	Mean	S.D.		
Delta	1.72	3.76	0.72	1.06	12.49	0.00001	1.37	2.94	0.75	1.22	7.41	0.007
Theta	0.68	1.60	0.17	0.64	17.02	0.00001	0.58	1.55	0.26	0.45	7.58	0.006
Alpha	1.45	1.90	0.12	0.73	83.28	0.0000001	1.31	1.64	0.32	0.82	56.11	0.0000001
Beta	0.19	0.39	−0.05	0.21	58.53	0.0000001	0.18	0.30	0.03	0.16	35.21	0.0000001

This prediction was tested by computing the absolute mean phase lag (i.e., $\sqrt{\theta^2}$ in msec) for all 189 subjects for each frequency band at different anterior-to-posterior and posterior-to-anterior interelectrode distances. Fig. 7 shows the mean absolute phase values at different interelectrode distances for the 4 EEG frequency bands. Two important features of the phase delay can be observed: (1) with the exception of the alpha frequency only a relatively small change in phase occurred between 7 and 14 cm, and (2) a non-linear relationship to phase was evident in all 4 frequency bands in which there was a marked increase in phase at 21 and 28 cm. This is consistent with the model that two different generators of coherence are operating, one involving short fibers and one involving long distance fibers. In support of this conclusion, the data were replotted in Fig. 8 with phase displayed as a function of EEG frequency at different interelectrode distances.

As with coherence, the rate of change of absolute phase with distance (i.e., the slope) was different in the posterior-to-anterior direction than in the anterior-to-posterior direction. Table III shows the slope mean and S.D. for the left and right hemisphere in the A-to-P and P-to-A directions. Statistically significant differences in slope were noted, with the greatest rate of change in absolute phase in the posterior-to-anterior direction as compared to the anterior-to-posterior direction.

Evidence for dispersive propagation

As described previously, phase is a function of frequency, distance and conduction velocity (Bendat and Piersol 1980). In the mathematics of wave mechanics, non-dispersive propagation refers to a linear relationship between frequency and conduction velocity. That is, when adjustments are made for relative phase then all frequencies propagate at the same velocity. In contrast, dispersive

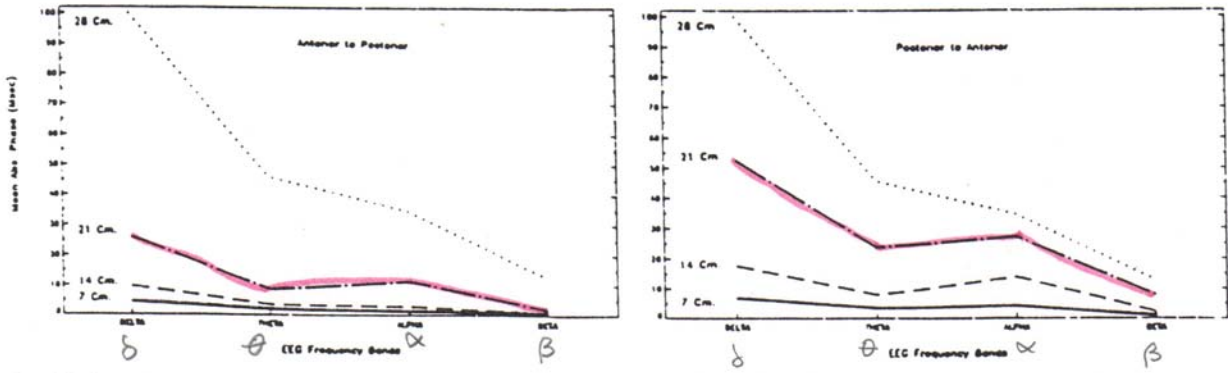

Fig. 8. Mean absolute phase (msec) in (A) the anterior-to-posterior and (B) posterior-to-anterior direction at different EEG frequenc bands. Averaged left and right hemisphere values (left + right)/2 are shown.

propagation is where phase is not a linear function of frequency, but instead will have a shape that defines the frequency dependence of the propagation. In other words, in a dispersive relationship different frequencies propagate at different velocities. In order to determine whether frequency propagation was dispersive the observed phase values were compared to an expected non-dispersive phase value. Non-dispersive phase values were computed by assuming that conduction velocity is constant and equal for all frequencies. Since distance is constant (i.e., 28 cm), non-dispersion is a direct ratio of the center frequencies of the autorecursive filters, i.e., $\vartheta_f/\delta_f = 2.125$; $\alpha_f/\delta_f = 4.5$; and $\beta_f/\delta_f = 9.5$. Bonferoni adjusted t tests (see Table IV) revealed that only the alpha frequency band was statistically different from the expected non-dispersive values in the posterior-to-anterior direction. It should be noted that the direction of deviation from non-dispersion is toward slower and not faster conduction velocities.

Differences in the magnitude of frequency dispersion between the anterior-to-posterior and posterior-to-anterior directions for different interelectrode distances were also analysed. As shown in Table IV, alpha exhibits a statistically significant dispersion relationship in the posterior-to-anterior direction but not in the anterior-to-posterior direction. This example of a spatial homogeneity of alpha dispersion is seen clearly in Fig. 7, where the slope of alpha phase with distance is much greater in the posterior-to-anterior than in the anterior-to-posterior direction (see Table III).

Discussion

Spherical volume conduction models of EEG assume spatial homogeneity in which the magnitude of voltage drops off rapidly with distance from the source. Correspondingly, a homogeneous model predicts that EEG coherence will decrease as a function of interelectrode distance with the decrement being equal in all directions. The results of the present study, however, do not support a homogeneous volume conduction model since considerable spatial inhomogeneity was noted. For example, the rate of change of coherence as a function of interelectrode distance was significantly different depending on the direction of change (i.e., posterior-to-anterior versus anterior-to-posterior) and the change in coherence was not a simple monotonic function of distance. Furthermore, there were significant differences in the

TABLE IV

Deviation from expected non-dispersion phase values at different interelectrode distances in the posterior-to-anterior versus the anterior-to-posterior directions

Distance (cm)	Frequency	Left hemisphere t tests		Right hemisphere t tests	
		P to A	A to P	P to A	A to P
7	Theta	0.72	0.67	1.62	−4.60
7	Alpha	6.17	2.58	7.69 *	0.06
7	Beta	1.14	5.30	3.11	1.21
14	Theta	−1.50	−2.94	0.45	−4.28
14	Alpha	10.02 **	2.84	10.71	2.77
14	Beta	1.46	−6.80	3.06	−1.45
21	Theta	−0.23	−6.68	6.83	−3.12
21	Alpha	13.26 **	6.17	12.72 **	6.44
21	Beta	4.05	−5.71	3.68	−2.00
28	Theta	−0.97	−0.97	−0.31	−0.31
28	Alpha	14.23 **	14.23 **	11.38 **	11.38 **
28	Beta	3.43	3.43	3.03	3.03

* P 0.001 (Bonteroni adjusted).
** P 0.0001 (Bonteroni adjusted).

magnitude of coherence between the anterior versus posterior regions and between left versus the right hemispheres. Since coherence is analogous to a squared cross-correlation coefficient, it is amplitude normalized and relatively independent of spectral intensity. This feature of coherence is important since known differences in EEG spectral intensity between the posterior versus anterior cannot account for the findings. This conclusion is bolstered by the corresponding differences in phase between the left versus right hemisphere and anterior versus posterior directions. Overall, these data demonstrate that there is considerable spatial inhomogeneity involved in the generation of coherence and that caution should be exercised in the application of volume conduction as a model of coherence. Instead, our data indicate that the contribution of various fiber systems must be considered in the formulation of any model of human EEG coherence.

Population competition and EEG coherence

Evidence for a competitive relationship between EEG generators was provided in the bivariate analyses that exhibited statistically significant negative linear and negative quadratic relationships (see Fig. 4C and D). The negative linear relationship indicates that as coherence increases within a local domain of cells, coherence decreases in a connected but spatially separate local domain. This is indicative of a competitive relationship in which there are shared connections between 'local' and 'long' distance systems. If we assume that there is a finite pool of neurons with local and long distance connections, then as the long distance connections dominate the output of a given pool of neurons there will be less influence by short distance connections. That is, increased coherence in one region of the cortex may be at the expense of coherence elsewhere in the cortex. A negative quadratic indicates a competitive relationship at the lower range of coherence where the slope is negative and a decoupling of the two local domains near the asymptote or when the slope approaches zero. It should be noted that the majority of significant bivariate relations were positive linear and/or positive quadratic, however, strong and reliable negative relationships were nonetheless present (Table II and Fig. 4C and D). These types of relationships are common in biological systems, although to our knowledge, they have not been reported in the case of EEG coherence. The presence of positive and negative linear or non-linear relationships between EEG generators emphasizes the need to develop a general model to explain the various short and long distance coherence relations observed in this study. In the sections to follow, a '2-compartmental' model of EEG coherence will be developed in an attempt to relate EEG coherence features observed at the scalp to the underlying neuroanatomy. This is one of the first attempts to relate neuroanatomy to EEG coherence in humans and the model is necessarily sketchy and incomplete. However, our intent is to explain as much of the observed spatial coherence findings as possible based on a single model. Our goal is to provide a detailed basis by which one may accept or reject the ideas proposed in the model.

Two-compartment model of EEG coherence

The 2-compartment model of EEG coherence proposes a mathematical relationship between cortical neuroanatomy, neurophysiology and the spatial properties of EEG coherence. The model is based on the Braitenberg's (1978) 2-compartment analysis of axonal fiber systems in which the apical dendrites of cortical pyramidal cells receive input primarily from 'long-range' connections from other pyramidal cells, while the basal dendrites receive input primarily from the axon collaterals from neighboring or 'local' pyramidal cells. These two architectonically distinct input circuits reflect the operation of two different systems: an 'A' system which is composed of basal dendrites, axon collaterals and metrically dependent, short-range connections and a 'B' system which is made up of apical dendrites, main axons, and non-metrically dependent cortico-cortical connections. The 'A' system primarily involves local interactions on the order of millimeters to a few centimeters, which occur primarily but not exclusively within the grey matter, while the 'B' system involves long-range interactions on the order of several centimeters which represent the majority of white matter fibers. These two systems (grey versus white

matter) exhibit two different network properties. System 'B' due to reciprocal connections and invariant apical dendrite terminations is involved in long distance feedback or loop systems, in contrast, system 'A' due to the variable depths of the basal dendrites is not involved in reciprocal loop processes but rather in a diffusion type of transmission process (Braitenberg 1978).

A diagrammatic representation of a 2-compartmental model of EEG coherence is shown in Fig. 9 in which P(1) and P(2) are two different populations of cells containing the individual elements x(1) and x(2) respectively. The elements of these two populations map to the elements in populations P(3) and P(4) (i.e., x(3) and x(4)) through a competitive network model involving excitatory (+) and inhibitor (−) inputs. This serial competitive feedback circuit represents the local connection compartment or system 'A.' The long distance fiber compartment is represented by the elements in populations P(1) and P(2) that map to the elements in populations P(5) and P(6) through an excitatory feedback loop. This compartment represents system 'B.' An important feature of this model is that it is non-linear involving contributions by two distinct compartments. A non-linear regression analysis of the experimental data was conducted using BMDP-3R in order to develop a mathematical formulation which can adequately account for the observed data. The non-linear equation was: coherence = $A_1e^{-kx} + A_2e^{kx}$ sin kx, where A_1 and A_2 and k are constants and x is interelectrode separation distance in cm. This equation was found to account for 99% of the variance of the interpolated alpha coherence measures obtained at 28 cm. The first term of the equation (A_1e^{-kx}) represents the exponential decrease with distance (x) of the density of local or system 'A' connections while the second term (A_2e^{kx}) represents the action of a feedback loop system with increasing distance (x) or system 'B' loop connections. In other words, the model is the sum of a negative exponential and a positive exponential function, where the negative exponential reflects the short fiber compartment (system 'A') in which the decay in coherence with distance is proportional to the density of short distance fibers and does not exhibit active feedback. The positive

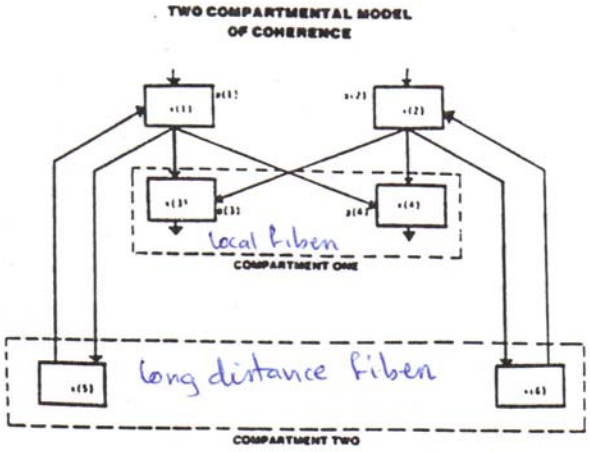

Fig. 9. A 2-compartmental model of cortical EEG coherence recorded from the scalp. Compartment one (C_1) represents the action of local fiber systems which exhibit dispersive properties and are best modeled by A_1e^{-kx} where A_1 is a constant of proportionality and x is interelectrode distance in cm. Compartment 2 (C_2) represents the action of long distance fiber systems which form feedback loops. This compartment is described by A_2e^{kx} sin x, where A_1, A_2 and k are constants and x is interelectrode distance in cm. Non-linear regression analysis showed that the following equation: coherence = $A_1e^{-kx} + A_2e^{kx}$ sin kx accounted for 99% of the variance of the observed coherence measures which supposedly reflect the non-linear summation of the 2 different fiber systems.

exponential and sine reflect the long distance fiber compartment (system 'B') which involves an excitatory loop process. According to this model, the curvilinear nature of the relation between the magnitude of coherence and electrode separation is a function of both the short and long distance fiber systems with the short distance fibers dominating the relationship at short distances and the long distance fibers becoming more dominate at longer distances.

The rate of change of coherence with distance and the magnitude of coherence between two points reflect two different features of the model. It is hypothesized that the rate of change is related to the density of short distance fibers in system 'A' and the magnitude is related to the density of long distance fibers of system 'B.' That is, the greater the complexity and competition of interaction between cells within a population, then the greater the average decrement of coherence as a

function of distance. The slope or fall-off of coherence is hypothesized to be a function of system 'A' since this system exhibits a diffusion type of spatial interaction. On the other hand, the longer distance fibers which travel primarily in the white matter involve excitatory couplings (Szentágothai 1978) and, therefore, the greater the density of couplings then the greater the magnitude of coherence. This distinction between the postulated system 'A' and 'B' coherence features allows for the concept of a short to long distance fiber ratio (S/L ratio). Such a hypothesized ratio can be computed by taking the ratio of the slope of change in coherence over a 7 cm (or less) distance to the magnitude of coherence over a 21 cm or greater distance.

Interhemispheric asymmetries

Coherence, independent of interelectrode spacing, was consistently greater from right hemisphere derivations than from left hemisphere locations. This finding is supported by the results of Tucker and colleagues (1982, 1984) demonstrating consistently greater right hemisphere coherence in comparison to the left hemisphere in both longitudinal and cross-sectional studies. If we assume that the density of white matter axons is related to the magnitude of scalp recorded coherence, then greater coherence in the right hemisphere in comparison to the left is consistent with studies (Gur et al. 1980) which show a higher white matter to grey matter ratio in the right hemisphere (i.e., more long distance fibers) in comparison to the left.

Studies by Thatcher et al. (1983) have demonstrated a negative relationship between coherence and intelligence in children. The results showed that increased coherence was strongly ($R^2 > 0.40$) associated with decreased intellectual functioning. These findings were interpreted in terms of a 'cerebral differentiation' model, in which decreased coherence was related to increased cortical differentiation in normal individuals [1]. According to this view, the increased right hemisphere coherence observed in the present study may be related to less cortical differentiation in the right hemisphere, relative to the left hemisphere. It would be consistent with the 2-compartment model to argue that the greater slope or change in coherence and absolute phase with distance in the left hemisphere in comparison to the right (see Tables I and III) is due to a higher ratio of short fiber interactions to long fibers (e.g., a higher density of interneurons) in the left hemisphere in comparison to the right. The critical concept is the ratio of short to long fibers (the S/L ratio) which determines the rate of change (or slope) of coherence with distance. According to the model the greater the S/L ratio the greater the slope of change in coherence and phase. This interpretation is supported by anatomical studies demonstrating that the left hemisphere is more highly fissured than the right (Connelly 1950) with a higher density of cells in the left than in the right hemisphere (Galaburda et al. 1978) as well as a larger planum temporale and longer sylvian fissure in the left hemisphere (Geschwind and Levitski 1968; Witelson and Pollie 1973; Chi et al. 1977). These findings, when taken as a whole, indicate that the organization of the left hemisphere favors processing or transfer within cortical regions, whereas the right hemisphere is more specialized for the processing or transfer of information across regions. This interpretation is consistent with established functional differences between the human left and right hemispheres (Kinsbourne 1974). Specifically, the left hemisphere has been shown to be strongly involved in analytical and sequential processing, which would presumably require a high degree of local differentiation and short distance interactions, whereas the right hemisphere is more involved in synthesis and relational functions which would require long distance fibers to coordinate and relate the outputs of the distributed local processors.

Anterior versus posterior asymmetries

Frontal regions consistently exhibited higher coherence than posterior regions. Furthermore, the rate of change in coherence and phase as a function of interelectrode separation was significantly less in the anterior-to-posterior direction than in

[1] As explained in Thatcher et al. (1983) this relationship holds only for neurologically intact individuals.

the posterior-to-anterior direction (Tables I and III). Based on the model, a lower slope of change can be interpreted as representing a lower density of short distance connections in compartment 'A.' This interpretation is supported by anatomical studies demonstrating an increased density of interneurons in posterior regions in comparison to anterior regions (Carpender and Sutin 1983). Also according to the model, an increase in the fall-off of coherence with distance (see Tables I and III and Fig. 2) is indicative of an increase in competitive interactions between local cell populations. In other words, an increase in the density of connections (number of connections/cm^2) between cells or small groups of cells in the posterior cortical regions favors an increase in competitive interactions and, as a consequence, there is a sharper fall-off in coherence and phase as a function of distance in the posterior-to-anterior direction than in the anterior-to-posterior direction.

The frontal regions were strongly coupled to occipital-parietal regions (see Table II and Fig. 5). A functional interpretation of this is that the organization of the frontal regions favors long distance connections, while the posterior regions are more involved in local processing. This is consistent with the functional role of frontal regions in action patterns and the planning and sequencing of goal-directed behavior which involves the integration and coordination of many specialized but spatially localized processes (e.g., processes caudal to the central sulcus related to vision, audition, somatosensory processing, language, etc.). Presumably, these functions of the frontal lobes would be subserved by long distance connections. This is in contrast to the role of posterior cortical regions which involve anatomically localized processing related to primary, secondary and tertiary perception and cognitive processes, which depend largely on local interactions.

Topographic patterns of coherence

Table II and Figs. 5 and 6 revealed distinct topographic patterns of coherence which are hypothesized to reflect specific cortico-cortical connection systems. The coherence patterns between F3-F4 and occipital-parietal regions in Fig. 5 suggest the operation of a long distance fronto-occipital fiber system (compartment 'B'). For example, the gross anatomy of the brain contains two long association fiber systems that interconnect frontal regions to occipital regions within the same hemisphere: (1) the uncinate fasciculus, and (2) the arcuate fasciculus (Carpender and Sutin 1983). It is hypothesized that one or both of these fiber systems are responsible for the observed coherence patterns between F3-F4 and occipital-parietal regions (see Table II and Fig. 5). Future studies with radial electrode arrays located in the occipital and frontal regions may be able to expand on these findings and provide more precise information about the conduction velocities and spatial distribution of the frontal-occipital fasciculi.

The intrahemispheric topographic coherence analyses (see Fig. 6) suggest several connection features. In general, midline regions (parietal-central, occipital-parietal and central-frontal) tended to be more locally connected (i.e., with minimal long distance connections) than the lateral regions (e.g., frontal-temporal and temporal-temporal). In contrast, the lateral regions tended to exhibit more long distance relations than did the medial regions (see Fig. 6). Finally, the temporal regions (i.e., T5-T3 and T6-T4) appear to possess a greater amount of connectivity in comparison to all other electrode combinations. That is, all other electrode combinations exhibited a statistically significant R^2 with the temporal electrodes, and the temporal regions exhibited the highest R^2 values in comparison to all other electrodes. This latter finding is consistent with the known anatomical connections of the temporal lobes in which cortical-limbic interactions occur through the entorhinal and subiculum pathways (Carpender and Sutin 1983). It is hypothesized that the observed coherence patterns involving the temporal regions in Fig. 6 reflect the influence of the convergent cortico-cortical connectivity of the temporal lobes.

Dispersion and the genesis of alpha rhythms

The presence or absence of a dispersion relationship is of critical importance since such information is necessary for the understanding of underlying wave mechanics. For example, Nunez

(1981) quantified the existence of a dispersive alpha frequency and used this information for the formulation of a wave model of EEG in general and alpha rhythms in particular. Nunez (1981), based on temporal and spatial frequency profiles, argued for the existence of at least two alpha generators or 'poles,' one located near the central regions (e.g., C3 and C4) and one located in the occipital-parietal regions. Differences in peak frequencies and spatial frequencies of the alpha rhythm from the central as opposed to the occipital-parietal regions supported this conclusion. In this context, the measures obtained in the present study further support the conclusions of Nunez (1981). For example, clear evidence for the existence of a dispersion relationship in the alpha frequency band was obtained (see Table IV and Figs. 7 and 8) which was of similar magnitude to that reported by Nunez (1981). Also, differences in the topography of alpha coherence (Fig. 3) and phase (Fig. 7) may be explained if one postulates

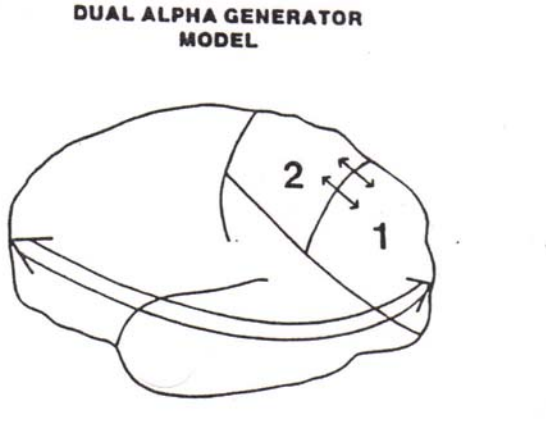

Fig. 10. A diagrammatic representation of a dual alpha generator system (areas 1 and 2). The alpha 'poles' are centered near the occipital region (1) and the central region (2). The 2 alpha systems compete for neuronal membership. The long arrow represents the occipital-frontal fiber pathways by which the frontal regions are driven at the alpha frequency by system 1, but not by system 2.

the existence of two alpha generator poles or regions in a similar manner as to that presented by Nunez (1981). Fig. 10 provides a diagrammatic model of a two alpha system capable of explaining differences in coherence and phase in the anterior-to-posterior versus posterior-to-anterior direction as well as the existence of the postulated fronto-occipital fiber system (compartment 'B'). For example, the alpha tuning characteristics observed in the anterior-to-posterior direction (see Fig. 3) may be explained if it is assumed that the frontal regions are driven primarily by the occipital-parietal alpha generator visa via the occipital-frontal pathways with minimal driving of the frontal regions by the central alpha generator. The lack of an alpha tuning peak at 7 and 14 cm in the posterior-to-anterior direction (see Fig. 3) may be explained if it is assumed that there is competition between the alpha generators located in the central and occipital regions, whereby alpha sources are synchronized principally by one or the other but not by both alpha generator systems. According to this interpretation the sudden appearance of an alpha tuning peak at 21 cm in the posterior-to-anterior direction (see Fig. 3) represents the influence of the long distance occipital fiber systems and reduced local competition in the frontal regions.

Finally, the greater magnitude of dispersion observed in the posterior-to-anterior direction in comparison to the anterior-to-posterior direction may be explained in either of two ways: (1) there is a lower mean conduction velocity in the posterior-to-anterior direction in comparison to the anterior-to-posterior direction, or (2) there is a greater mean density of cellular interaction in the posterior-to-anterior direction and thus a greater mean transmission delay in the posterior-to-anterior direction. We tend to reject explanation number 1 since, to our knowledge, there is no evidence of a directional asymmetry in fasciculi conduction velocities. In contrast, explanation number 2 is supported by anatomical evidence that clearly demonstrates a markedly increased density of interneurons in posterior cortical regions in comparison to the frontal cortical regions (Carpender and Sutin 1983). In other words, it is hypothesized that the unidirectional decrease in alpha conduc-

tion velocity (see Table IV) is due to greater interneuronal competition and greater interneuronal interaction in the posterior-to-anterior direction than in the anterior-to-posterior direction.

Résumé

Associations cortico-corticales et cohérence EEG: un modèle à deux compartiments

La cohérence EEG a été calculée pour 19 localisations sur le scalp de 189 enfants d'âge variant entre 5 et 16 ans. Des tests d'homogénéité spatiale de la cohérence EEG ont été effectuées en comparant la cohérence EEG en fonction des différentes distances interélectrodes dans les directions antéro-postérieure et postéro-antérieure. Des nonhomogénéités très significatives ont été observées, puisqu'une plus grande cohérence était présente en direction antéro-postérieure que dans l'autre direction. Une plus grande cohérence était également observée dans les dérivations frontales, par rapport aux dérivations postérieures, et dans l'hémisphère droit par rapport à l'hémisphère gauche. Ces données indiquent la présence d'au moins deux sources différentes de cohérence EEG: (1) une cohérence produite par l'action des connexions axonales courtes et (2) une cohérence produite par l'intermédiaire de connexions longues. Les mesures des délais de phase en fonction de la distance interélectrode sont en accord avec un modèle de cohérence EEG à 'deux compartiments', où des caractéristiques différentes de cohérence sont engendrées par des systèmes de fibres de longueurs différentes.

We gratefully acknowledge the assistance of Dr. William Chapin for suggesting the phase test of the model and Dr. David Cantor for reading earlier drafts. We also extend our appreciation to Neurometrics, Inc. for providing some of the data acquisition and analysis software.

This research was supported by USDA Grant HRD0200 and NIH-MBS Grant RR096110 to R.W. Thatcher, principal investigator.

References

Beaumont, J.G., Mayes, A.R. and Rugg, M.D. Asymmetry in EEG alpha coherence and power: effects of task and sex. Electroenceph. clin. Neurophysiol., 1978, 45: 393–401.

Beaumont, J.G. and Rugg, M.D. The specificity of intrahemispheric EEG alpha coherence asymmetry related to psychological task. Biol. Psychol., 1979, 9: 237–248.

Bendat, J.S. and Piersol, A.G. Engineering Applications of Correlation and Spectral Analysis. Wiley, New York, 1980.

Braitenberg, V. Comparison of different cortices as a basis for speculation on their functions. In: H. Petsche and M.A.B. Brazier (Eds.), Synchronization of EEG Activity in Epilepsies. Springer, New York, 1972: 47–63.

Braitenberg, V. Thoughts on the cerebral cortex. J. theoret. Biol., 1974, 46: 421–447.

Braitenberg, V. Cortical architectonics: general and areal. In: M.A.B. Brazier and H. Petsche (Eds.), Architectonics of the Cerebral Cortex. Raven Press, New York, 1978: 443–465.

Busk, J. and Galbraith, G.C. EEG correlates of visual-motor practice in man. Electroenceph. clin. Neurophysiol., 1975, 38: 415–422.

Cantor, D.S., Thatcher, R.W., McAlaster, R., Lester, M.L. and Horst, R.L. Topographic distribution of EEG hemispheric coherence related to cognitive functioning in children. Southeastern Conf. on Human Development, 1982, abstr.

Carpender, M.B. and Sutin, J. Human Neuroanatomy. Williams and Wilkins, Baltimore, MD, 1983.

Chi, J.G., Dooling, E.S. and Gilles, F.H. Gyral development of the human brain. Ann. Neurol., 1977, 1: 86–94.

Connelly, C.J. External Morphology of the Primate Brain. Thomas, Springfield, IL, 1950.

Dixon, W. and Brown, M. Biomedical Computer Programs P-Series. University of California Press, Berkeley, CA, 1979.

Dudley, B.A.C. Mathematical and Biological Interrelations. Wiley, New York, 1977.

Flor-Henry, P., Kiles, Z.J. and Tucker, D.M. Studies in EEG power and coherence (8–13 Hz) in depression mania and schizophrenia compared to controls. Adv. biol. Psychiat., 1982, 9: 1–7.

Galaburda, A.M., LeMay, M., Kemper, T.L. and Geschwind, N. Right–left asymmetries in the brain. Science, 1978, 199: 852–856.

Geschwind, N. and Levitski, W. Human brain: left–right asymmetries in temporal speech region. Science, 1968, 161: 186–187.

Glaser, E.M. and Ruchkin, D.S. Principles of Neurobiological Signal Analysis. Academic Press, New York, 1976.

Globus, A. and Scheibel, A.B. Pattern and field in cortical structure: the rabbit. J. comp. Neurol., 1967, 131: 155–172.

Gur, R.C., Packer, I.K., Hungerbuhler, J.P., Reivich, M., Obrist, W.D., Amarnek, W.S. and Sackeim, H.A. Differences in the distribution of gray and white matter in human cerebral hemispheres. Science, 1980, 207: 1226–1228.

Jasper, H.H. The ten-twenty electrode system of the International Federation. Electroenceph. clin. Neurophysiol., 1958, 10: 371–375.

Kinsbourne, M. Mechanisms of hemisphere interaction in man In: M. Kinsbourne and L. Smith (Eds.), Hemispheric Disconnection and Cerebral Function. Thomas, Springfield IL, 1974: 71–86.

Krieg, W.J.S. Connections of the Cerebral Cortex. Brain Books Chicago, IL, 1963.